First publ. in : Organometallics ; 31 (2012), 24. - S. 8505-8515
DOI : 10.1021/om300755j

Controlled Acrylate Insertion Regioselectivity in Diazaphospholidine-Sulfonato Palladium(II) Complexes

Philipp Wucher,[†] Philipp Roesle,[†] Laura Falivene,[‡] Luigi Cavallo,[§] Lucia Caporaso,*[,‡] Inigo Göttker-Schnetmann,[†] and Stefan Mecking*[,†]

[†]Chair of Chemical Materials Science, Department of Chemistry, University of Konstanz, Universitätsstrasse 10, 78457 Konstanz, Germany

[‡]Department of Chemistry, University of Salerno, Via Ponte Don Melillo, 84084 Fisciano, Salerno, Italy

[§]Kaust Catalysis Center, Chemical and Life Sciences and Engineering, King Abdullah University of Science and Technology, Thuwal 23955-6900, Saudi Arabia

Supporting Information

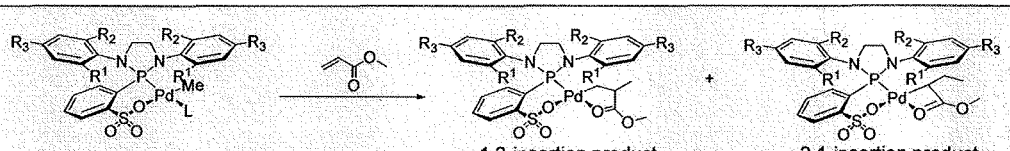

a: R_1 = H, R_2 = H, R_3 = H	< 5 %	**> 95 %**
b: R_1 = CH_3, R_2 = H, R_3 = H	50 %	50 %
c: R_1 = OCH_3, R_2 = H, R_3 = H	50 %	50 %
d: R_1 = CH_3, R_2 = CH_3, R_3 = CH_3	**93 %**	7 %
e: R_1 = $CH(CH_3)_2$, R_2 = $CH(CH_3)_2$, R_3 = H	**> 95 %**	< 5 %
f: R_1 = (C_6H_4-*p*CH_3), R_2 = (C_6H_4-*p*CH_3), R_3 = H	**> 95 %**	< 5 %

ABSTRACT: Diazaphospholidine-sulfonato Pd(II) complexes [{κ^2-*P,O*-(*N*-$Ar_2C_2H_4N_2P$)$C_6H_4SO_3$}PdMe(L)] **1**-L (L = dmso, pyridine, lutidine, or μ-LiCl(solvent); **1a**: Ar = Ph, **1b**: Ar = 2-MeC_6H_4, **1c**: Ar = 2-$MeOC_6H_4$, **1d**: Ar = 2,4,6-$Me_3C_6H_2$, **1e**: Ar = 2,6-*i*$Pr_2C_6H_3$, **1f**: Ar = 2,6-(*p*-tolyl)$_2C_6H_3$) were prepared and structurally characterized. The regioselectivity of methyl acrylate (MA) insertion into the Pd–Me bond is entirely inverted from >93% 1,2-insertion for bulky substituents (**1d–f**, yielding the insertion products [(P^O)Pd{κ^2-*C,O*-CH_2CHMeC(*O*)OMe], **12**) to the usual electronically controlled 2,1-insertion (>95%) for the less bulky Ar = Ph (**1a**, yielding the insertion product [(P^O)Pd{κ^2-*C,O*-CHEtC(*O*)OMe], **11**, and β-H elimination product methyl crotonate). DFT studies underline that this is due to a more favorable insertion transition state (2,1- favored by 12 kJ mol^{-1} over 1,2- for **1a**) vs destabilization of the 2,1-insertion transition state in **1d,e**. By contrast, MA insertion into the novel isolated and structurally characterized hydride and deuteride complexes [{κ^2-*P,O*-(*N*-$Ar_2C_2H_4N_2P$)$C_6H_4SO_3$}PdR(lutidine)] (Ar = 2,6-*i*$Pr_2C_6H_3$; **9e**: R = H, **10e**: R = D) occurs 2,1-selectively. This is due to the insertion occurring from the isomer with the P-donor and the olefin in *trans* arrangement, rather than the insertion into the alkyl from the *cis* isomer in which the olefin is in proximity to the bulky diazaphospholidine. **1a–f** are precursors to active catalysts for ethylene polymerization to highly linear polyethylene with M_n up to 35 000 g mol^{-1}. In copolymerization experiments, norbornene was incorporated in up to 6.1 mol % into the polyethylene backbone.

INTRODUCTION

The selective insertion of an olefinic substrate into a metal–carbon bond is a decisive step in many catalytic transformations. In the area of polymer synthesis, this is impressively illustrated by isotactic polypropylene. Its properties ultimately result from a highly regio- and stereoselective insertion of propylene into the growing chain. By comparison to the large-scale application of catalytic polymerization of apolar olefins such as ethylene and propylene,[1] an insertion (co)polymerization of electron-deficient monomers such as acrylates is challenging. Considerable progress in this area has been achieved by the development of d^8-metal (late transition metal) complexes. Their less oxophilic nature, in comparison to their early transition metal counterparts, renders them more tolerant toward polar moieties.[2] Thus, cationic palladium and nickel α-diimine complexes **3** (Figure 1) can copolymerize ethylene and 1-olefins with acrylates, yielding branched copolymers.[3] Due to the propensity of the cationic Pd(II) catalysts for "chain walking" by a series of rapid β-hydride elimination and reinsertion events, the polymers formed are highly branched, with the acrylate-derived repeat units located at the end of branches.

In contrast, highly linear ethylene-methyl acrylate copolymers without any chain-walking-derived microstructure are obtained with neutral Pd(II) complexes **2**-L based on anionic phosphine-

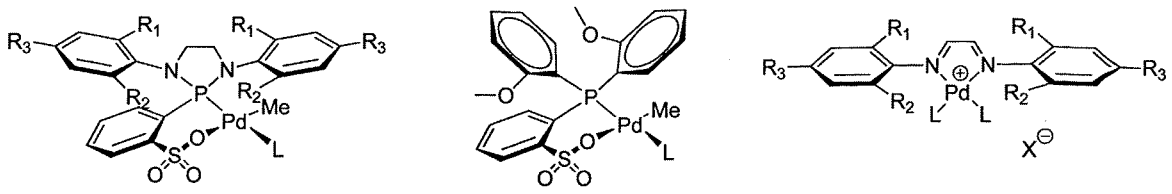

Figure 1. Neutral diazaphospholidine-sulfonato Pd(II) complexes (left), neutral phosphine-sulfonato Pd(II) complex (center), and cationic Pd(II) diimine complexes (right).

Scheme 1. Preparation of Diazaphospholidine-Pd(II) Complexes

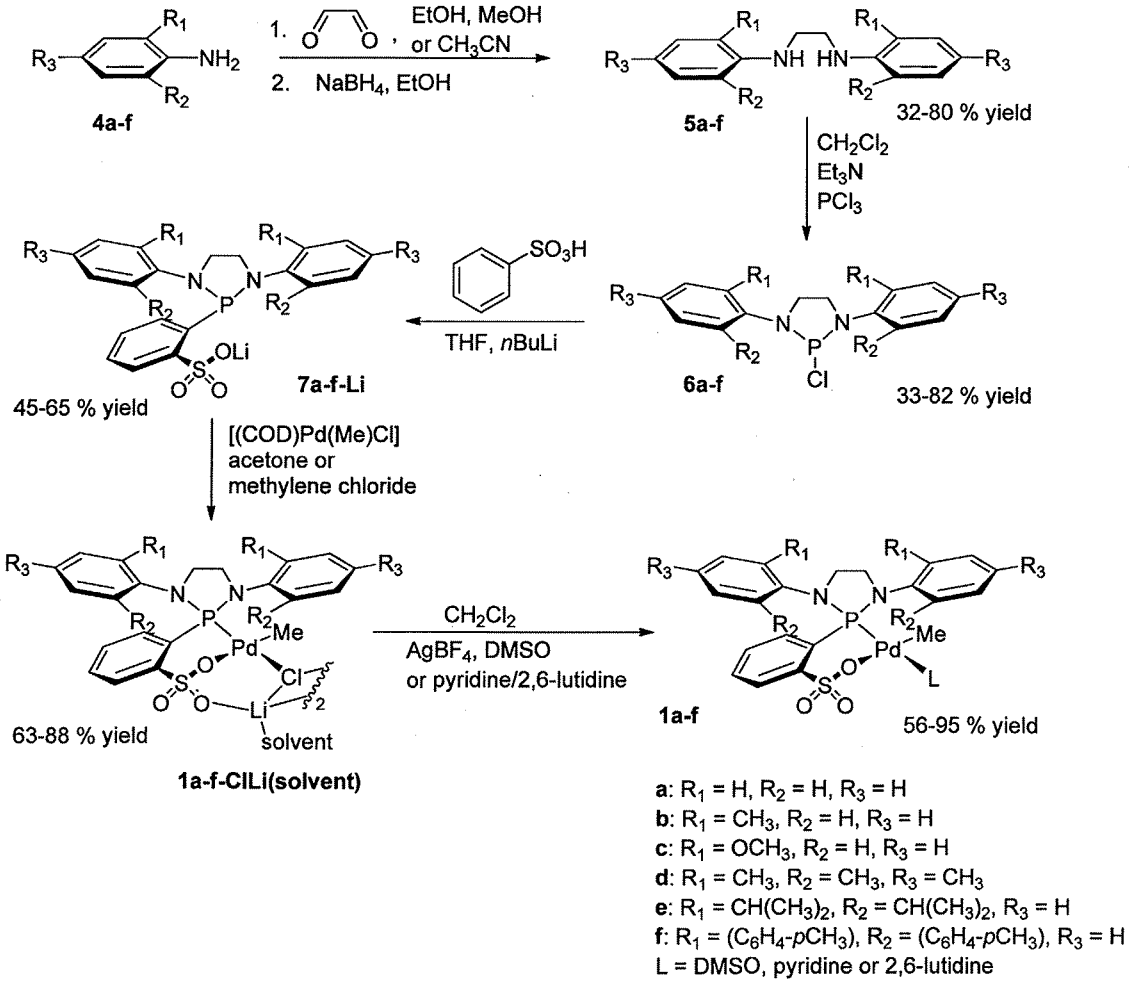

a: R_1 = H, R_2 = H, R_3 = H
b: R_1 = CH_3, R_2 = H, R_3 = H
c: R_1 = OCH_3, R_2 = H, R_3 = H
d: R_1 = CH_3, R_2 = CH_3, R_3 = CH_3
e: R_1 = $CH(CH_3)_2$, R_2 = $CH(CH_3)_2$, R_3 = H
f: R_1 = (C_6H_4-*p*CH_3), R_2 = (C_6H_4-*p*CH_3), R_3 = H
L = DMSO, pyridine or 2,6-lutidine

sulfonato ligands $[\{\kappa^2\text{-}P,O\}\text{-}(2\text{-}MeOC_6H_4)_2PC_6H_4SO_2O]^-$. A variety of polar comonomers in addition to methyl acrylate (MA), e.g., vinyl ether, acrylonitrile, vinyl fluoride, acrylamides, vinyl acetate, vinyl sulfones, acrylic acid, substituted norbornenes, and allyl acrylate, have been effectively copolymerized with ethylene by complexes of type **2**.[2i,4,5] These unique catalytic properties can be related to the unsymmetric nature of the anionic chelating ligand, with a soft phosphine and a hard sulfonate oxygen donor.[6] With respect to influencing the olefin insertion step, however, the immediate environment of the metal center is rather open in these square-planar complexes: the sulfonate donor bears little steric bulk, and the aryl substituents on the phosphorus donor of **2** point away from the metal center. We have recently communicated that by incorporation of the P-donor into a diazaphospholidine heterocycle, with N-bound aryl moieties, the latter can be forced into closer proximity to the metal center to invert the regioselectivity of acrylate insertion.[7]

We now give a full account of the insertion behavior and catalytic properties of this class of complexes.

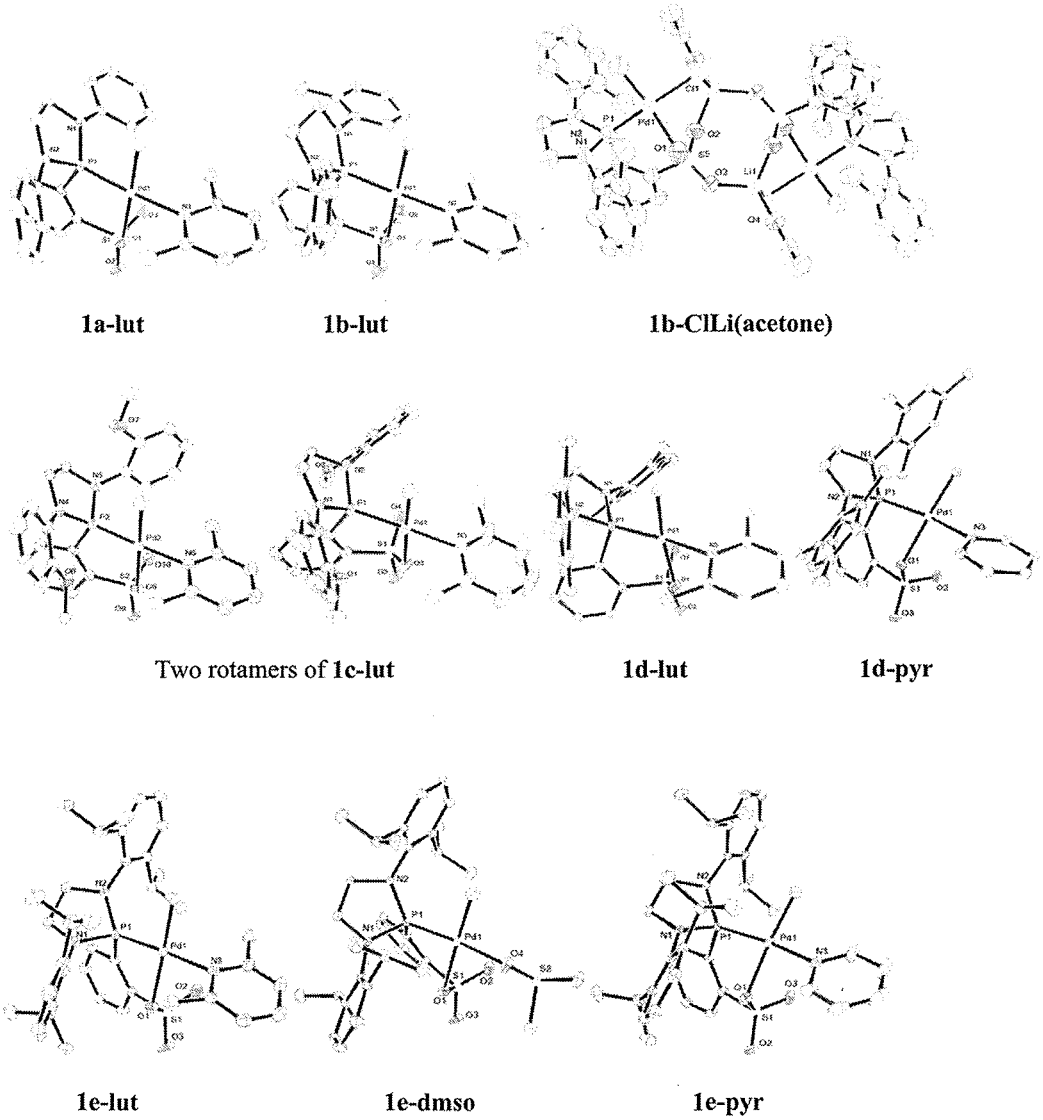

Figure 2. ORTEP plot of complexes **1a**-lut, **1b**-lut, **1b**-ClLi(acetone), **1c**-lut, **1d**-lut, **1d**-pyr, **1e**-lut, **1e**-dmso, and **1e**-pyr drawn with 50% probability ellipsoids. All hydrogen atoms and cocrystallized solvent molecules are omitted for clarity.

RESULTS AND DISCUSSION

Preparation of Diazaphospholidine Ligands and Complexes. Diazaphospholidine-sulfonates with various *N*-aryl substitution patterns and their Pd(II) complexes were prepared similarly to the procedures reported previously for **1d**-L and **1e**-L.[7] The diamines **5** were prepared in a two-step reaction in 32% to 80% yield, starting with the condensation of glyoxal and aniline derivative **4**, followed by reduction of the intermediate diimines with $NaBH_4$. The isolated diamines **5** were reacted with PCl_3 in the presence of an excess of triethylamine to yield the 2-chloro-diazaphospholidines **6**,[8] which were further reacted with *o*-dilithiobenzenesulfonate to form the anionic ligands **7**. These lithium salts form the LiCl-bridged binuclear Pd(II) complexes **1a**-ClLi(acetone), **1b**-ClLi(acetone), **1c**-ClLi(acetone), and **1f**-ClLi(MeOD) in 63% to 88% yield by a stoichiometric reaction with [(1,5-cyclooctadiene)Pd(Me)Cl][9] (Scheme 1). The corresponding mononuclear dimethylsulfoxide complexes **1**-dmso can be prepared by addition of equimolar amounts of $AgBF_4$ and DMSO to a methylene chloride solution of the chloride-bridged complexes **1**-ClLi(solvent). Addition of the stronger coordinating pyridine or 2,6-lutidine without additional silver salts results in the direct formation of the corresponding mononuclear pyridine or lutidine complexes **1**-pyr and **1**-lut in 56% to 95% yield. All ligands and complexes were fully characterized by 1D- and 2D-NMR spectroscopy and elemental analysis (see Supporting Information).

In addition, X-ray diffraction analyses of complexes **1a**-lut, **1b**-lut, **1c**-lut, **1d**-lut, **1d**-pyr, **1e**-lut, **1e**-dmso, **1e**-pyr, and **1b**-ClLi(acetone) (Figure 2) confirm their identity. Complexes **1a**-lut and **1c**-lut crystallize in the triclinic $P\bar{1}$ space group, whereas **1b**-lut, **1d**-lut, **1d**-pyr, **1e**-lut, **1b**-ClLi(acetone), and **1e**-dmso crystallize in the monoclinic $P2_1/c$ or $C2/c$ space group. All complexes exhibit a square-planar environment around the Pd

Table 1. Selected Bond Distances for Diazaphospholidine Complexes 1-L

	Pd–L [Å]	Pd–P [Å]	Pd–O [Å]	Pd–C [Å]
1a-lut	2.134(6)	2.191(7)	2.147(5)	2.030(0)
1b-lut	2.134(0)	2.197(3)	2.141(5)	2.048(7)
1c-lut	2.120(7)/2.119(7)	2.191(3)/2.190(6)	2.147(7)/2.151(2)	2.034(7)/2.028(2)
1d-lut	2.139(2)	2.228(6)	2.153(4)	2.027(8)
1d-pyr	2.107(7)	2.205(7)	2.165(4)	2.032(2)
1d-dmso[7]	2.149(6)	2.187(9)	2.159(6)	2.187(9)
1e-lut	2.136(9)	2.212(8)	2.174(9)	2.018(9)
1e-pyr	2.112(2)	2.202(8)	2.178(2)	2.021(7)
1e-dmso	2.129(8)	2.179(1)	2.181(2)	2.019(3)

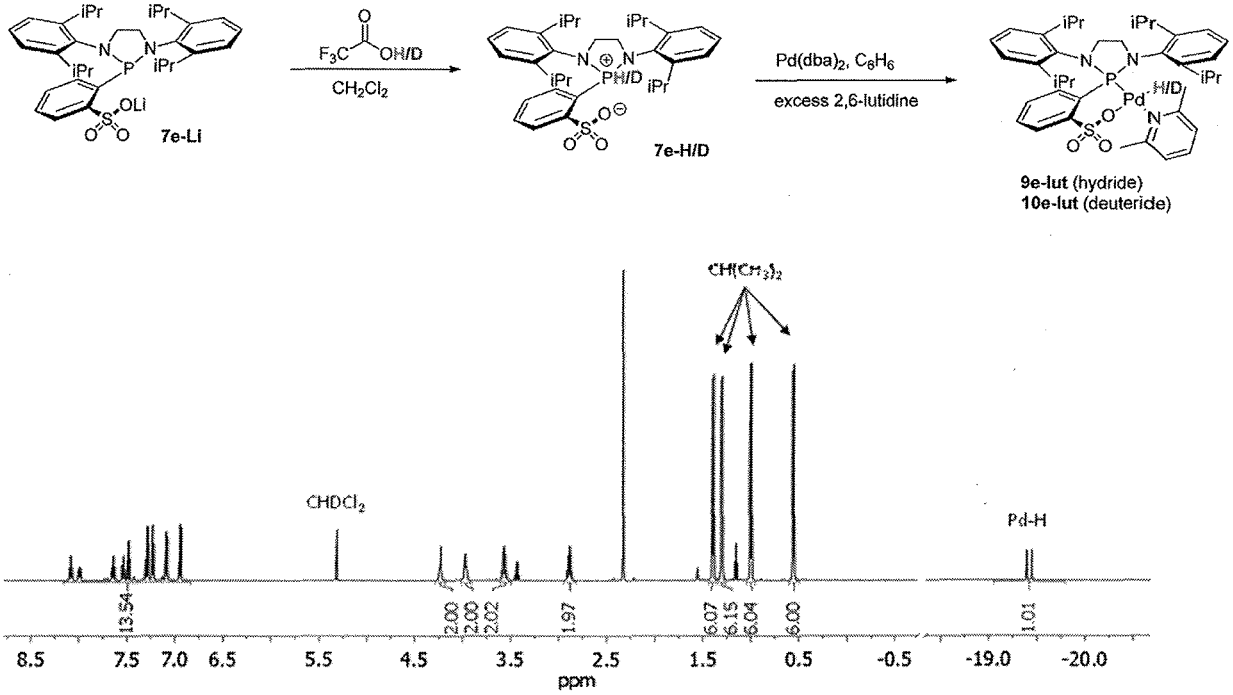

Figure 3. Synthesis of **9e**-lut and ^{1}H NMR spectrum (400 MHz, CD_2Cl_2, 298 K) of **9e**-lut.

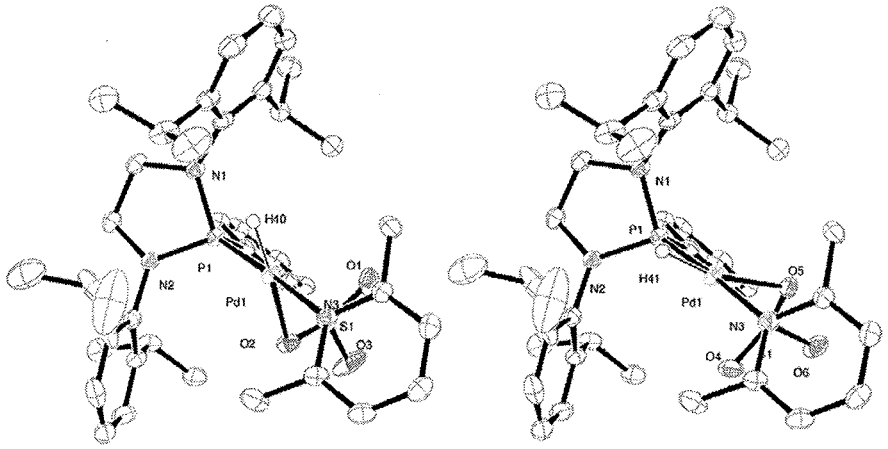

Figure 4. ORTEP plots of two rotamers (rotational disorder of the sulfonate group and the hydride atom) of **9e**-lut drawn with 50% probability ellipsoids. Hydrogen atoms (except Pd-H) are omitted for clarity. Hydrides H40 and H41 were located in the electron density map after the other hydrogen atoms were treated as a riding model. Selected bond length [Å]: Pd1–H40 1.559(0), Pd1–H41 1.514(7), Pd1–N3 2.125(3), Pd1–P1, 2.176(8), Pd1–O2 2.190(5), Pd1–O5 2.230(6).

Scheme 2. Regioselectivity of Insertion of Methyl Acrylate into a Pd–Me Bond of Complex 1-L

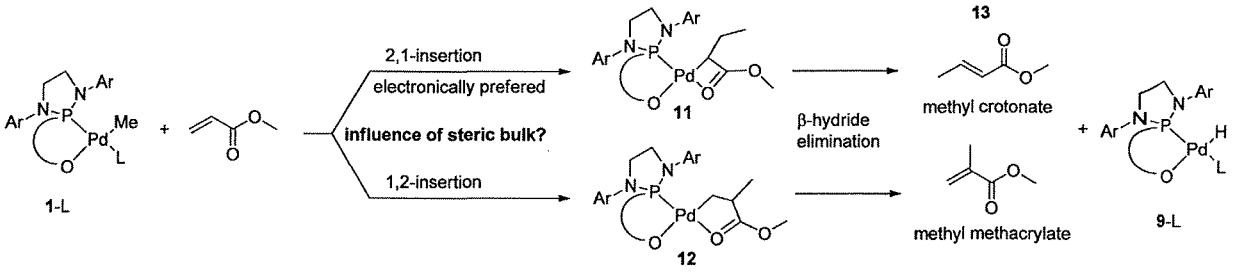

Scheme 3. Observed Regioselectivity of Diazaphospholidine Sulfonato Pd(II) Complexes 1a–f with MA

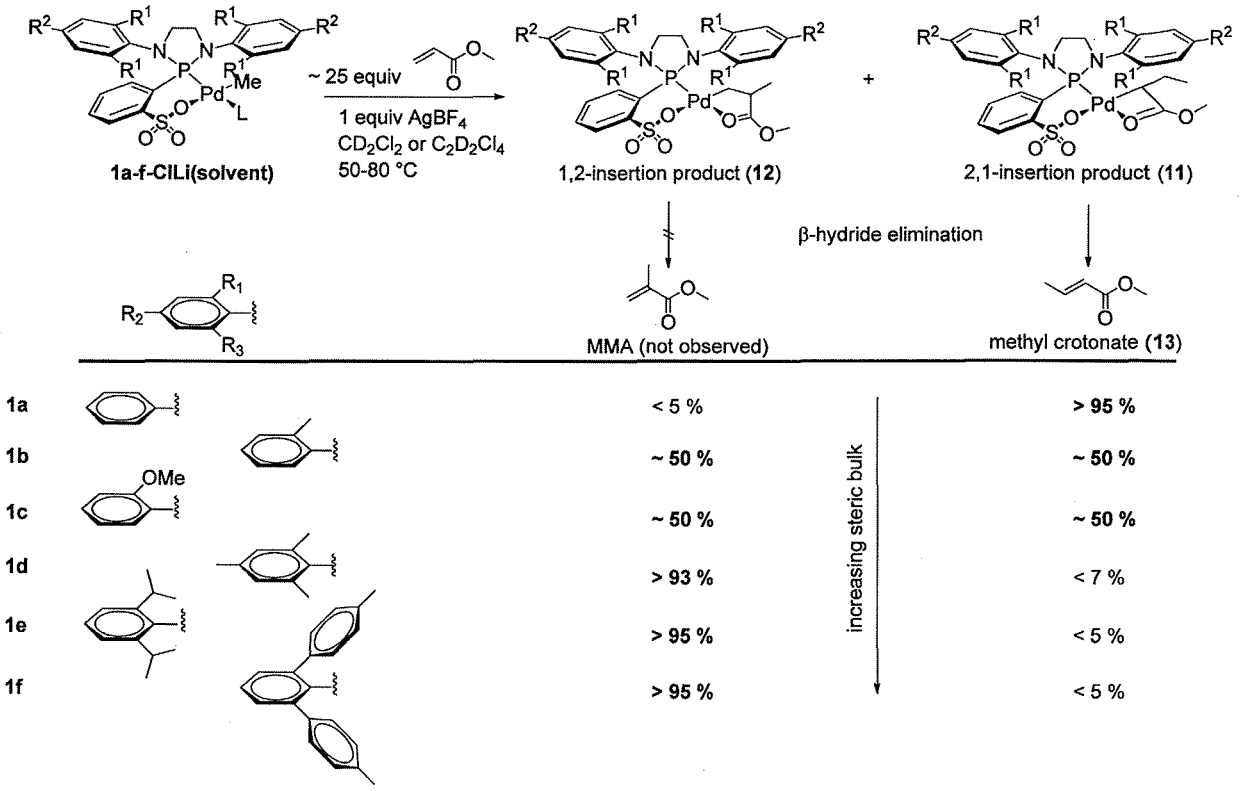

center, with the methyl group and the phosphorus atom located mutually *cis* to each other. The crystal structure of complex **1**c-lut contains two rotamers per unit cell, with both methoxy-anisyl groups occupying the same and the opposite site, respectively, of the diazaphospholidine ring.

The bond lengths around the Pd atom (Table 1) are all in the expected range, with palladium phosphorus distances between 2.18 and 2.22 Å.[10] For the 2,6-lutidine-coordinated complexes **1**a–e-lut, the Pd–N and the Pd–P distances increase slightly in the order *o*-MeO < Ph < *o*-Tol < *i*Pr < Mes from 2.120 Å to 2.139 Å and from 2.191 Å to 2.228 Å, respectively. Concerning the effect of the labile ligand L, the Pd–P distance (*trans* to the labile ligand) elongates in the order dmso < pyridine < 2,6-lutidine since dmso exerts less of a *trans* influence on the phosphorus atom than an N-donor. Furthermore, dmso exhibits κ-*O* coordination to the Pd(II) center in the solid-state structure of **1**d-dmso[7] and **1**e-dmso, which is in contrast to the phosphine-sulfonato Pd(II) complex [(κ^2-*P,O*)-*P*[*o*-(2′-6′-$(OMe)_2C_6H_3$)-C_6H_4]$_2$(*o*-SO_2O-C_6H_4)PdMe]-dmso, where dmso was found to bind κ-*S*.[4b]

In addition to these palladium methyl complexes **1**-L, the Pd-hydride and Pd-deuteride complexes **9**e-lut and **10**e-lut (Ar = iPr_2Ph) were synthesized by oxidative addition of P-protonated (**7**e-H) or deuterated ligand (**7**e-D), respectively, to [$Pd^0(dba)_2$] in the presence of excess 2,6-lutidine (Figure 3). The deuteride complex **10**e-lut contained about 30% of the corresponding hydride complex **9**e-lut, indicated by the characteristic high-field ^{1}H NMR resonance of the hydride at −19.42 ppm (see Supporting Information).

Crystals of **9**e-lut suitable for single-crystal X-ray diffractometry were grown by layering a solution of the complex in acetone with pentane in an NMR tube (Figure 4). The crystal structure shows a rotational disorder of the sulfonate group, which was modeled by two sets of oxygen positions, O1, O2, O3 and O4, O5, O6, refining to an occupancy of 61:39. After modeling this disorder the split hydride positions H40 and H41

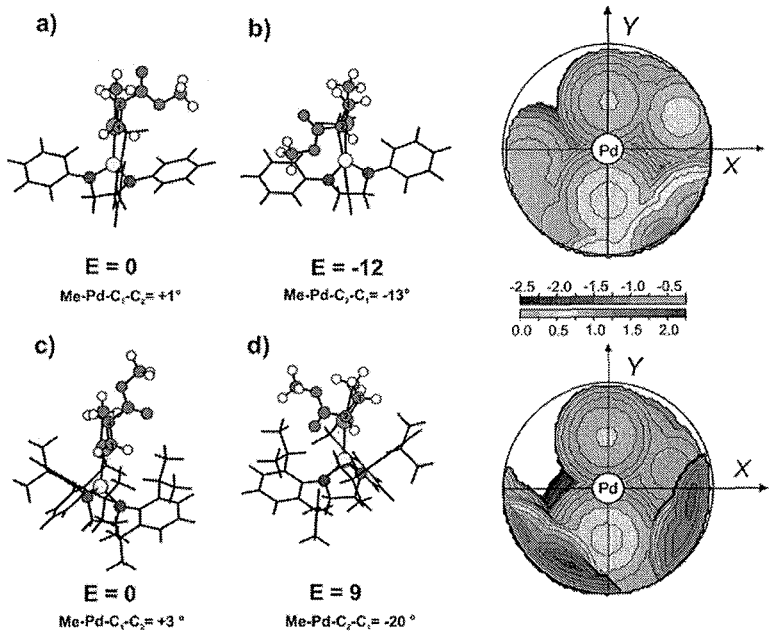

Figure 5. Transition-state geometries of 1,2-insertion [left: a and c] and 2,1-insertion [middle: b and d] of MA into fragments **1a** (top) and **1e** (bottom). Right: Steric maps of fragments **1a** and **1e**. The colored scale indicates the isocontour levels, in angstroms. Orientation of the ligands in the steric maps as in (a) and (b), (c) and (d). Data for fragment **1e** were taken from ref 7. Energies in kJ mol^{-1}.

were located in the electron density map, while all other hydrogen atoms were refined by use of a riding model. As in the other crystallized diazaphospholidine-sulfonato complexes (vide supra), the labile neutral monodentate ligand 2,6-lutidine is coordinated *trans* to the phosphorus atom.

Regiochemistry of Insertion. For polar vinyl monomers, the regioselectivity of insertion into a transition metal carbon bond, and in particular a palladium–carbon bond, is usually electronically controlled. This applies to polymerization as well as transition metal catalyzed cross-coupling reactions.[2i,11] Thus, electron-deficient olefins such as methyl acrylate selectively insert in a 2,1-fashion,[3,4,12] whereas electron-rich olefins such as vinyl ethers have a strong preference for 1,2-insertion.[5a,13,14]

As we have shown previously in a combined experimental and computational study,[7] the regiochemistry of insertion of electron-deficient polar monomers such as methyl acrylate can be inverted from an electronically preferred 2,1- to a 1,2-insertion by an appropriately arranged steric bulk of the ligand. Complexes **1e**-ClLi(acetone) and **1d**-ClLi(acetone) yielded the "regioirregular" 1,2-insertion product **12** in over 93% NMR yield, due to a destabilization of the transition state of 2,1-insertion. This proposed concept of sterical destabilization of the transition state of 2,1-insertion also implies that by decreasing the steric bulk of the ligand, the insertion should be electronically controlled to favor the 2,1-insertion product (**11**) of MA into the Pd–CH_3 bond of diazaphospholidine-sulfonato complexes **1**-L, which upon β-hydride elimination, yield methyl crotonate (**13**) and the corresponding hydride complex **9**-L (Scheme 2).

To this end, the reaction of the electron-deficient polar olefin methyl acrylate toward the sterically less demanding complexes **1a**-ClLi(acetone), **1b**-ClLi(acetone), and **1c**-ClLi(acetone) was monitored by NMR spectroscopy. To a methylene chloride-d_2 solution of the complex (30 μmol in 0.6 mL), one equivalent of silver tetrafluoroborate and 20 to 25 equivalents of MA were added. The silver-mediated chloride abstraction took place within minutes at room temperature, and the reaction mixture was monitored by proton NMR spectroscopy at 50 °C. In all cases, the Pd-CH_3 signal decreases and a simultaneous increase of characteristic signals for 2,1- and 1,2-insertion was observed.[15] β-Hydride elimination after 2,1-insertion to methyl crotonate (**13**) took place immediately after some 2,1-insertion product **11** had formed, whereas the 1,2-insertion product **12** was stable under these conditions. Due to this complex reaction scheme, only the decrease of the Pd-CH_3 signal could be analyzed by a linear fit for a pseudo-first-order reaction. The obtained rate constants at 50 °C are $k_{obs} = (5.0 \pm 0.1) \times 10^{-5}\ s^{-1}$, $k_{obs} = (3.7 \pm 0.1) \times 10^{-5}\ s^{-1}$, and $k_{obs} = (1.2 \pm 0.1) \times 10^{-4}\ s^{-1}$ for the decay of the Pd-CH_3 signal of **1a**-ClLi(acetone), **1b**-ClLi(acetone), and **1c**-ClLi-(acetone), respectively. These numbers compare to the reported values of **1d**-ClLi(actone) at 25 °C and **1e**-ClLi(thf) at 45 °C of $k_{obs} = (6.0 \pm 0.1) \times 10^{-4}\ s^{-1}$ and $k_{obs} = (4.8 \pm 0.1) \times 10^{-4}\ s^{-1}$, respectively.[7]

A quantitative analysis of the formed insertion products **12** (after 1,2-insertion) and methyl crotonate (**13**) (after 2,1-insertion and β-hydride elimination) by ^{1}H NMR spectroscopy reveals that a decrease of the steric bulk of the *N*-aryl moieties in diazaphospholidine-sulfonato palladium methyl complexes **1**-L indeed inverts the insertion regiochemistry of methyl acrylate from 1,2-insertion (**1d**-L and **1e**-L)[7] to 2,1-insertion: The observed ratios of **12** to methyl crotonate (**13**) are 20:1 (for **1d**, **1e**), ca. 1:1 (for **1b**, **1c**), and 1:23 (for **1a**) (Scheme 3).

Complex **1f**-ClLi(CD_3OD) was not stable after silver-mediated chloride abstraction and decomposed during the insertion experiment at 50 °C, evident by the rapid formation of palladium black. Therefore, the more stable pyridine complex **1f**-pyr was investigated in its reactivity toward MA. Insertion of MA into the Pd–methyl bond was monitored in $C_2D_2Cl_4$ via proton NMR spectroscopy at elevated temperature (80 °C). The Pd-CH_3 signal decays under these conditions with a pseudo-first-

Scheme 4. Possible Insertion Pathways of MA into the Pd(II)-Hydride Complex 9e-lut

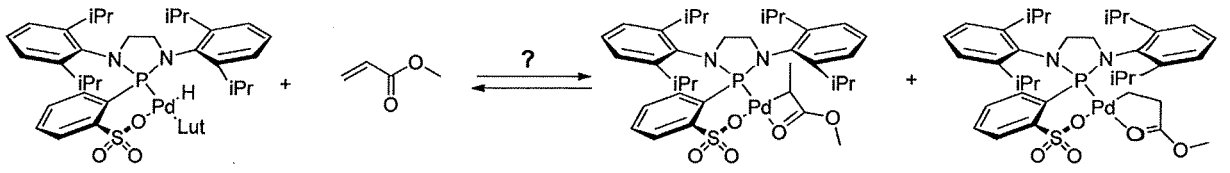

Scheme 5. Reaction of 10e-lut with 12 Equivalents of MA in C_6D_6 at Room Temperature[a]

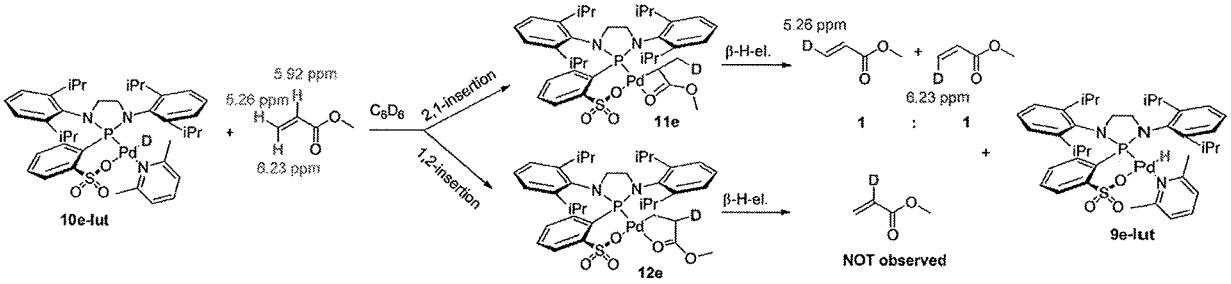

[a]Exclusive 2,1-insertion of methyl acrylate into **10e**-lut is proven by H/D exchange only at the terminal position of methyl acrylate.

order rate constant of $k_{obs} = (1.2 \pm 0.1) \times 10^{-4}\ s^{-1}$, while only the formation of the 1,2-insertion product was observed.

The observed ratios of 1,2- and 2,1-insertion are in qualitative agreement with density functional theory calculations at the BP86 generalized gradient approximation level[16] performed on some of these complexes. MA insertion proceeds by η^2-coordination of MA to the palladium(II) center *trans* to the phosphorus donor atom, followed by *cis–trans* isomerization, and insertion in the less stable *cis* isomer.

Previous calculations revealed that the mesityl and 2,6-diisopropylphenyl moieties of fragments **1d** and **1e** are in close proximity to the methoxycarbonyl group of the incoming MA substrate, which forces the latter to rotate out of plane. This destabilizes the Cossée–Arlmann-like transition state of the electronically preferred 2,1-insertion. As a result, the transition state of 1,2-insertion is kinetically favored over the transition state of 2,1-insertion by an energy difference of 3 and 9 kJ mol^{-1} for the fragments **1d** (*N*-aryl = mesityl) and **1e** (*N*-aryl = 2,6-diisopropylphenyl), respectively.[7]

DFT calculations for fragment **1a** (*N*-aryl = phenyl) now confirm that for this sterically less constrained metal center indeed the transition state for 2,1-insertion of methyl acrylate is favored by 12 kJ mol^{-1} over 1,2-insertion (Figure 5). This agrees with the experimentally observed regiochemistry of methyl acrylate insertion into **1a** (vide supra). Further calculations for an *N*-methyl-substituted diazaphospholidine show that for this even smaller substituent 2,1-insertion is even more pronouncedly favored (18 kJ mol^{-1} vs 1,2-insertion), which further illustrates the role of these substituents for regioselectivity (cf. Supporting Information, Figure S7.3).

The influence of the appropriately arranged steric bulk of the ligands of complexes **1a** (Ar = phenyl) and **1e** (Ar = 2,6-diisopropylphenyl) on the transition state of MA insertion is illustrated in the calculated steric maps (Figure 5). Fragment **1a** features a very flat topology, which shows no strong influence of steric factors.

Besides the two aforementioned opposite insertion products and the β-hydride elimination product methyl crotonate, the formation of palladium black was observed during reaction overnight. This implies that the investigated diazaphospholidine-sulfonato complexes are somewhat unstable under these conditions. Also, in all cases, no insertion of MA into a Pd–hydride bond, which should be present in the reaction mixture after β-hydride elimination, was observed. To further elucidate this issue, the reactivity of the isolated hydride complex **9e**-lut toward MA was studied. NMR spectroscopic monitoring of a solution of **9e**-lut and MA in CD_2Cl_2 at 40 °C did not provide any evidence of an insertion, even at prolonged reaction times (overnight). Only slow decomposition by reductive elimination, evidenced by the formation of palladium black and the lutidinium salt of the diazaphospholidine ligand **7e** ($[\{N\text{-}(2,6\text{-}i\text{Pr}_2C_6H_3)_2C_2H_4N_2P\}C_6H_4SO_3]^-[C_7H_{10}NH]^+$), was observed. Even with a large excess of MA (ca. 200 equiv), no insertion products were observed over a wide temperature range studied (−80 to 25 °C).

When, however, the analogous deuteride complex **10e**-lut is reacted with 12 equivalents of MA in benzene-d_6, an immediate increase of the Pd-hydride signal from 30% (from **9e**-lut as an impurity in the deuteride complex, vide supra) to over 90% is observed within a few minutes at room temperature. Also, the phosphorus resonance at 88.39 ppm, a 1:1:1 triplet with a coupling constant of 3.6 Hz ($^2J_{P-D}$), decreases in favor of a distinct doublet at 88.18 ppm with a coupling constant of 26.4 Hz ($^2J_{P-H}$). This clearly shows that insertion into the Pd–D/H bond takes place very rapidly, but since no insertion product was detected, immediate β-hydride elimination appears to be even faster such that the insertion/elimination equilibrium is on the side of the hydride complex **9e**-lut and free MA (Scheme 4).

^2H NMR spectroscopy of the reaction mixture in C_6D_6 revealed the nature of the previous insertion mode. Only two resonances, at 5.26 and 6.23 ppm, for the terminal olefin, but no resonance for the internal olefin (expected at 5.91 ppm) were observed. This clearly shows that only 2,1-insertion into the Pd–D bond of **10e**-lut occurs (Scheme 5). The intermediate formation of the electronically favored 2,1-insertion product is further backed up by the observed ingrowth of two triplets at

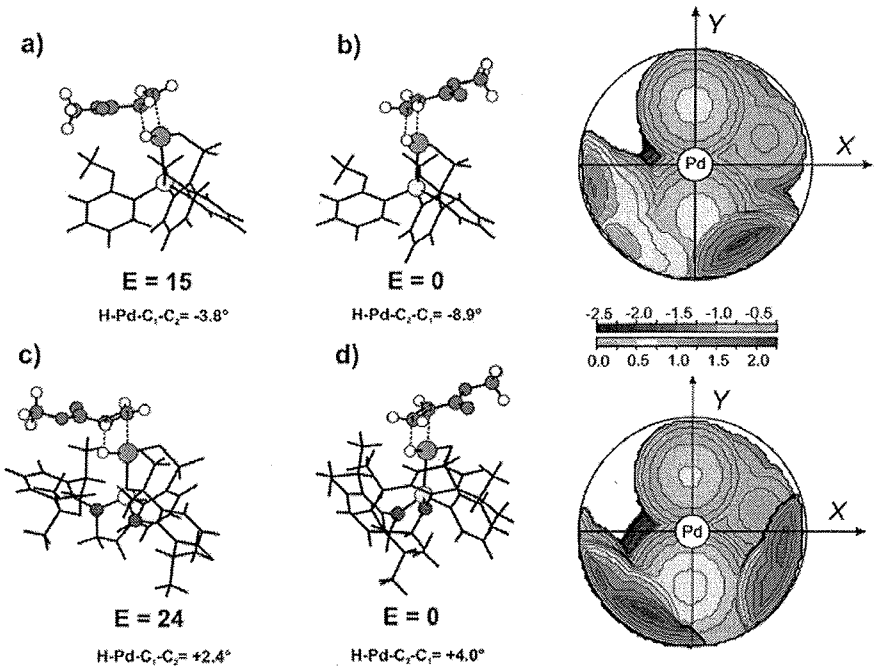

Figure 6. Transition-state geometries for MA insertion in phosphine-sulfonato Pd(II) hydride complex (top) in 1,2-mode (a) and 2,1-mode (b). MA insertion into diazaphospholidine-sulfonato Pd(II) hydride complex **9e**-MA (bottom) in 1,2-mode (c) and 2,1-mode (d). Right: Steric maps of the ligand spheres of complex **2** (top) and **1e**/**9e** (bottom). The colored scheme for the isocontour profiles, in Å, is reported on the right. Orientation of the ligands in the steric maps as in (a) and (b), (c) and (d). Energies in kJ mol^{-1}.

130.3 ppm with a characteristic coupling constant of 24.7 Hz ($^1J_{C-D}$) in the ^{13}C NMR spectrum of a stoichiometric reaction of **10e**-lut and MA in CH_2Cl_2. The ^2H NMR spectrum of this stoichiometric reaction mixture features the terminal olefinic resonances (6.38 and 5.83 ppm in CH_2Cl_2) and the Pd-deuteride complex **10e**-lut (−19.32 ppm) in a statistical ratio of approximately 1:1:1 (see Supporting Information).

This 2,1-insertion of methyl acrylate into the palladium hydride bond of **10e**-lut is unexpected since methyl acrylate insertion into the corresponding palladium methyl fragment **1e** proceeds with 1,2-insertion regioselectivity.[7] The origin of this opposite reactivity was revealed by DFT studies. For the methyl complexes **1e**-MA and **2**-MA, in agreement with calculations reported for **2**-MA[17] and for **1e**-MA,[7] methyl acrylate initially coordinates *trans* to the phosphorus atom, then undergoes a *trans* to *cis* isomerization. Insertion proceeds from this *cis*-coordinated intermediate since the corresponding *cis* transition state is lower in energy than the *trans* transition state (Figure S7.6, top).[7,17] The regioselectivity is controlled by the steric bulk of the ligand, and the 2,1-insertion mode is disfavored by 9 kJ mol^{-1} vs the 1,2-insertion for **1e** (vide supra).[7] In the case of the hydride or deuteride complex (**9e**-MA or **10e**-MA), consistently with Nozaki's results on the olefin insertion into the hydride complex analogous to **2**,[17b] calculations reveal that the *trans* transition state for 2,1-insertion of MA is favored over the *cis* transition state (Figure S7.5 and Figure 6). As a consequence, reaction occurs by MA coordination *trans* to the phosphorus atom[18] followed by 2,1-insertion from this *trans* geometry (Figure S7.6, bottom). In other words, no *trans* to *cis* isomerization is necessary. In the *trans* complex, 1,2-insertion is disfavored by 24 kJ mol^{-1} vs 2,1-insertion (Figure 6). Due to the cooperative electronic and steric effects (see Figure 6, steric maps), this difference in insertion barrier is higher compared to the related phosphine-sulfonato system **2** (15 kJ mol^{-1}).

Ethylene Homopolymerization Studies. Beyond these stoichiometric studies of insertion, the catalytic properties of complexes **1**-L were studied. All compounds are precursors to active catalysts for ethylene homopolymerization (Table 2). Productivities are limited by comparison to the phosphine-sulfonato complex **2**-L (L = dmso, pyridine, 2,6-lutidine) at comparable conditions.[4] The low activity also arises from a reduced stability at elevated temperatures for the diazaphospholidine complexes, particularly **1d**-L and **1e**-L, as evidenced by a decreasing ethylene uptake with time during polymerization experiments (Figure 7).

Complexes **1d**-lut (Ar = mesityl) and **1e**-lut (Ar = 2,6-$iPr_2C_6H_3$) for example exhibit their highest productivity at 50 °C (Table 2, entries 2−18 and 2−24), whereas complexes **1a**-lut (Ar = phenyl) and **1b**-lut (Ar = *o*-tolyl) reach their highest productivity of 2.0 × 10^3 mol_{C2H4} mol_{Pd}^{-1} and 3.6 × 10^3 mol_{C2H4} mol_{Pd}^{-1}, respectively, at 90 °C (Table 2, entries 2-3 and 2-14). The terphenyl-substituted complex **1f-pyr** did not yield significant amounts of polymer.

As expected, complexes of the weaker coordinating ligand DMSO display higher activities (compare for example entries 2-3 and 2-8 or entries 2-18 and 2-21), as it competes less with monomer binding by comparison to lutidine or pyridine. Also, higher ethylene pressure leads to an increase in catalyst activity (compare entries 2-4 and 2-6).

Molecular weights of the isolated polymers depend strongly on the diazaphospholidine aryl substitution pattern. The least bulky complex **1a**-lut (Ar = phenyl) produced polyethylene with a molecular weight of up to 35 000 g mol^{-1}, which is on the same order of magnitude as found for the phosphine-sulfonato

Table 2. Ethylene Polymerization by Neutral Diazaphospholidine-Sulfonato Pd(II) Complexes 1-L[a]

entry	cat. precursor	pressure [bar]	temperature [°C]	yield [mg]	TON [(mol C_2H_4) (mol Pd)$^{-1}$]	M_n[c] [g mol^{-1}]
2-1	**1a**-lut	10	50			
2-2	**1a**-lut	10	70	40	146	n.d.
2-3	**1a**-lut	10	90	275	984	34 600
2-4	**1a**-lut	5	90	167	599	30 900
2-5	**1a**-lut	20	90	354	1268	38 300
2-6	**1a**-lut	40	90	534	1909	35 900
2-7	**1a**-dmso[b]	10	70	40	650	n.d.
2-8	**1a**-dmso[b]	10	90	120	1948	24 300[d]
2-9	**1b**-lut	10	50	46	167	2580
2-10	**1b**-lut	10	70	131	468	1800
2-11	**1b**-lut	10	90	103	369	1800
2-12	**1c**-lut	10	50			
2-13	**1c**-lut	10	70	91	326	
2-14	**1c**-lut	10	90	501	1793	27 500
2-15	**1c**-lut	5	90	277	991	19800
2-16	**1c**-lut	20	90	748	2673	20 200
2-17	**1c**-lut	40	90	944	3372	20 000
2-18	**1d**-lut	10	50	900	3217	1000
2-19	**1d**-lut	10	70	784	2800	600
2-20	**1d**-lut	10	90	428	1531	600
2-21	**1d**-dmso[b]	10	50	278	4513	1500
2-22	**1d**-dmso[b]	10	70	64	1039	1200[d]
2-23	**1e**-lut	10	40	983	3514	900
2-24	**1e**-lut	10	50	1397	4992	700
2-25	**1e**-lut	10	70	1109	3964	600
2-26	**1e**-lut	20	50	1430	5107	700
2-27	**1f**-lut	10	50	n.d.		
2-28	**1f**-lut	10	90	63	228	4400

[a]Reaction conditions: 100 mL of toluene, 30 min reaction time, 10 μmol of Pd(II). [b]2.2 μmol of Pd(II). [c]Determined by ^{1}H NMR in $C_2D_2Cl_4$ at 130 °C. [d]Determined by GPC in 1,2,4-trichlorobenzene at 160 °C vs linear polyethylene.

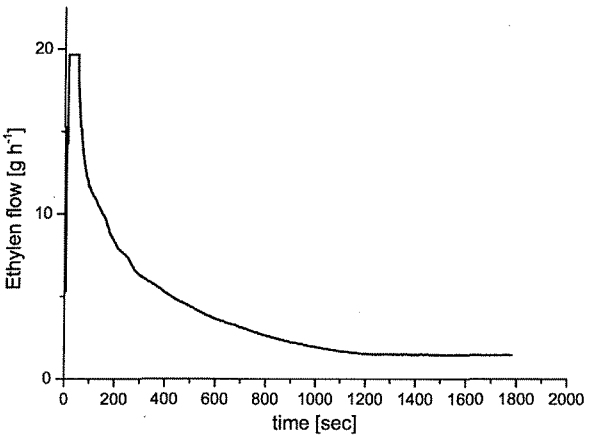

Figure 7. Typical mass flow plot of ethylene homopolymerization with **1e**-lut (20 μmol of Pd, 100 mL of toluene, 50 °C, 10 bar of ethylene, 30 min).

complexes **2**. The more bulky complexes **1d**-lut (Ar = mesityl) and **1e**-lut (Ar = 2,6-*i*Pr$_2$C$_6$H$_3$) are more active (vide supra), but produce oligomeric material with molecular weights of about 1000 g mol^{-1} or less. This is somewhat unexpected since it is thought that more bulky ligands increase catalyst activity and molecular weight of polyethylene produced by phosphine-sulfonato Pd(II) complexes,[19] although this is not a clear trend.[20] The electron-donating methoxy group of complex **1c**-lut enhances productivity and molecular weight compared to the methyl-substituted complex **1b**-lut (compare entries 2-11 and 2-14).

All catalyst precursors produce highly linear polyethylenes according to quantitative high-temperature ^{13}C NMR spectroscopy. Only for polyethylenes formed by **1a**-lut and **1b**-lut a small amount of methyl branches was detectable, two methyl branches per 1000 carbon atoms, but no higher alkyl branches were found.

Copolymerization Studies. The most active catalyst, **1e**-lut, was also studied in copolymerization experiments of ethylene and various comonomers, namely, methyl acrylate, styrene, norbornene, 5-norbornene-2,3-dicarboxylic anhydride, vinyl acetate, and vinyl ether (Table 3). Only the strained norbornene was incorporated (Table 3, entries 3-6 and 3-7), while in the presence of all other comonomers polyethylene homopolymer was formed. Molecular weights of these polyethylenes are between 600 and 900 g mol^{-1}, which is in the same range as in ethylene homopolymerization in the absence of comonomers. Taking into account these molecular weights, the detection limit of the aforementioned composition analysis is less than one comonomer repeat unit per chain. That is, even comonomer-derived end groups can be excluded. The polymer yield decreased significantly in the presence of polar-substituted comonomers by comparison to polymerization without comonomer (entry 3-1). This decrease in productivity is likely due to competing σ-coordination of the polar moiety, as observed in detailed studies of the phosphine-sulfonato complexes **2**.[21] This interpretation is also supported by the finding that the presence of styrene did not reduce the yield as

Table 3. Results of Polymerization in the Presence of Ethylene and Various Comonomers by 1e-lut[a]

entry	comonomer	$C_{Comonomer}$ [mol L^{-1}]	yield [mg]	TON ethylene [(mol C_2H_4) (mol Pd)$^{-1}$]	TON comon. [(mol X) (mol Pd)$^{-1}$]	incorp. comon. [mol %]	M_n[b] [g mol^{-1}]
3-1			2950	4213			900
3-2	methyl acrylate	0.1 M	544	777		<0.1%	1000
3-3	methyl acrylate	0.3 M	303	433		<0.1%	1000
3-4	styrene	0.1 M	1869	2670		<0.1%	800
3-5	styrene	0.3 M	1275	1821		<0.1%	800
3-6	norbornene	0.1 M	1744	2404	26	3.5%	700
3-7	norbornene	0.3 M	2325	3119	60	6.1%	700
3-8	5-norbornene-2,3-dicarboxylic anhydride	0.1 M	744	1063		<0.1%	700
3-9	5-norbornene-2,3-dicarboxylic anhydride	0.3 M	293	418		<0.1%	600
3-10	vinyl acetate	0.05 M	535	764		<0.1%	800
3-11	vinyl acetate	0.1 M	312	446		<0.1%	900
3-12	ethyl vinyl ether	0.05 M	413	590		<0.1%	900
3-13	ethyl vinyl ether	0.1 M	194	277		<0.1%	800

[a]Reaction conditions: 100 mL total volume (comonomer + toluene), 30 min reaction time, 50 °C, 25 μmol of **1e**-lut, 10 bar of ethylene, 200 mg of BHT. [b]Determined by ^{1}H NMR in $C_2D_2Cl_4$ at 130 °C.

pronouncedly (entries 3-4 and 3-5) and that productivity decreases with increasing concentration of the polar comonomer.

Copolymerizations of ethylene with 0.1 and 0.3 mol L^{-1} norbornene (entries 3-6 and entry 3-7) yielded oligomeric materials as highly viscous oils with a molecular weight (by ^{1}H NMR) of about 700 g mol^{-1} and a norbornene content of 3.5 and 6.1 mol %, respectively. Isolated norbornene units are incorporated into the linear ethylene backbone.[22] This incorporation of norbornene is about four times lower compared to phosphine-sulfonato complexes **2**, which produced copolymers with 48 000 g mol^{-1} and 12 mol % norbornene incorporation under similar conditions (24 μmol of Pd, 0.1 mol L^{-1}, 20 bar).[23] In general, the steric bulk of the diazaphospholidine moiety appears to hamper incorporation of comonomer vs ethylene incorporation.

SUMMARY AND CONCLUSIONS

This comprehensive study of new diazaphospholidine-sulfonato Pd(II) complexes reveals that within this class of compounds the regioselectivity of acrylate insertion can be inverted via the bidentate ligand. Depending on the steric bulk of the *N*-aryl substituents, insertion can occur very selectively (>95%) in either a 2,1- or 1,2-fashion. This is due to a destabilization of the 2,1-insertion transition state by interference of bulky substituents with the coordinated acrylate substrate that overrides the electronic preference for this insertion mode,[7] while for less sterically demanding substituents the 2,1-insertion transition state was found to be energetically favorable vs the transition state of 1,2-insertion by DFT studies. In stark contrast, acrylate insertion into diazaphospholidine hydride (or deuteride) complexes was observed to follow the common 2,1-insertion pathway even for very bulky substituted complexes (R = 2,6-iPr$_2$C$_6$H$_3$). Theoretical studies reveal the origin of this different behavior. Other than insertion into a metal–alkyl bond, insertion into the hydride occurs from the species in which the π-coordinated acrylate is *trans* to the P-donor, with the hydride in *cis* position. Thus, the olefin is more remote from the P-donor and its substituents, and the insertion step is less sensitive to their steric bulk. All representatives of diazaphospholidine-sulfonato complexes studied were found to be active for ethylene polymerization. In the presence of various comonomers, under polymerization conditions, incorporation of ethylene is much preferred. This chemoselectivity can be related to a preference for the less bulky ethylene monomer.

ASSOCIATED CONTENT

Supporting Information

Supplemental tables and figures, CIF files, general experimental procedures, synthesis, additional NMR spectra, crystal structures, Cartesian coordinates, and energies of DFT calculations. This material is available free of charge via the Internet at http://pubs.acs.org.

AUTHOR INFORMATION

Corresponding Author

*Fax: +49 7531 88-5152. Tel: +49 7531 88-5151. E-mail: stefan.mecking@uni-konstanz.de; lcaporaso@unisa.it.

Notes

The authors declare no competing financial interest.

ACKNOWLEDGMENTS

Financial support by the DFG (Me1388/10-1) is gratefully acknowledged. The authors thank Lars Bolk for GPC, Anke Friemel and Ulrich Haunz for support with NMR measurements, and the HPC team of Enea (www.enea.it) for use of the ENEA-GRID and the HPC facilities CRESCO (www.cresco.enea.it) in Portici, Italy.

REFERENCES

(1) Mülhaupt, R. *Macromol. Chem. Phys.* **2003**, *204*, 289–327.

(2) (a) Ittel, S. D.; Johnson, L. K.; Brookhart, M. *Chem. Rev.* **2000**, *100*, 1169–1203. (b) Gibson, V. C.; Spitzmesser, S. K. *Chem. Rev.* **2003**, *103*, 283–316. (c) Mecking, S. *Coord. Chem. Rev.* **2000**, *203*, 325–351. (d) Mecking, S. *Angew. Chem., Int. Ed.* **2001**, *40*, 534–540. (e) Guan, Z. *Chem. Eur. J.* **2002**, *8*, 3086–3092. (f) Domski, G. J.; Rose, J. M.; Coates, G. M.; Bolig, A. D.; Brookhart, M. *Prog. Polym. Sci.* **2007**, *32*, 30–92. (g) Berkefeld, A.; Mecking, S. *Angew. Chem., Int. Ed.* **2008**, *47*, 2538–2542. (h) Chen, E. Y.-X. *Chem. Rev.* **2009**, *109*, 5157–5214. (i) Nakamura, A.; Ito, S.; Nozaki, K. *Chem. Rev.* **2009**, *109*, 5215–5244.

(3) (a) Johnson, L. K.; Mecking, S.; Brookhart, M. *J. Am. Chem. Soc.* **1996**, *118*, 267–268. (b) Mecking, S.; Johnson, L. K.; Wang, L.; Brookhart, M. *J. Am. Chem. Soc.* **1998**, *120*, 888–899. (c) Johnson, L. K.; Bennett, A.; Dobbs, K.; Hauptamnn, E.; Ionkin, A.; McCord, E.;

McLain, S.; Radzewich, C.; Yin, Z.; Wang, L.; Wang, Y.; Brookhart, M. *Polym. Mater. Sci. Eng.* **2002**, *86*, 319.
(4) (a) Drent, E.; van Dijk, R.; van Ginkel, R.; van Oort, B.; Pugh, R. I. *Chem. Commun.* **2002**, 744–745. (b) Guironnet, D.; Roesle, P.; Rünzi, T.; Göttker-Schnetmann, I.; Mecking, S. *J. Am. Chem. Soc.* **2009**, *131*, 422–423.
(5) (a) Luo, S.; Vela, J.; Lief, G. R.; Jordan, R. F. *J. Am. Chem. Soc.* **2007**, *129*, 8946–8947. (b) Weng, W.; Shen, Z.; Jordan, R. F. *J. Am. Chem. Soc.* **2007**, *129*, 15450–15451. (c) Skupov, K. M.; Piche, L.; Claverie, J. P. *Macromolecules* **2008**, *41*, 2309–2310. (d) Ito, S.; Munakata, K.; Nakamura, A.; Nozaki, K. *J. Am. Chem. Soc.* **2009**, *131*, 14606–14607. (e) Bouilhac, C.; Rünzi, T.; Mecking, S. *Macromolecules* **2010**, *43*, 3589–3590. (f) Rünzi, T.; Guironnet, D.; Göttker-Schnetmann, I.; Mecking, S. *J. Am. Chem. Soc.* **2010**, *132*, 16623–16630. (g) Rünzi, T.; Fröhlich, D.; Mecking, S. *J. Am. Chem. Soc.* **2010**, *132*, 17690–17691. (h) Daigle, J.-C.; Piche, L.; Claverie, J. P. *Macromolecules* **2011**, *44*, 1760–1762. (i) Daigle, J.-C.; Piche, L.; Arnold, A.; Claverie, J. P. *ACS Macro Lett.* **2012**, *1*, 343–346.
(6) Nozaki, K.; Kusumoto, S.; Noda, S.; Kochi, T.; Chung, L. W.; Morokuma, K. *J. Am. Chem. Soc.* **2010**, *129*, 16030–16042.
(7) Wucher, P.; Caporaso, L.; Roesle, P.; Ragone, F.; Cavallo, L.; Mecking, S.; Göttker-Schnetmann, I. *Proc. Natl. Acad. Sci. U. S. A.* **2011**, *108*, 8955–8959.
(8) Abrams, M. B.; Scott, B. L.; Baker, R. T. *Organometallics* **2000**, *19*, 4944–4956.
(9) Rülke, R. E.; Ernsting, J. M.; Spek, A. L.; Elsevier, C. J.; van Leeuwen, P. W. N. M.; Vrieze, K. *Inorg. Chem.* **1993**, *32*, 5769–5778.
(10) Pd–N and Pd–P distances of phosphine-sulfonato Pd(II) lutidine and pyridine complexes: Pd–P: 2.2 Å, Pd–N: 2.1 Å; ref 20. For further examples cf. refs 5a, d, 6, 11, and 19.
(11) Beletskaya, I. P.; Cheprakov, A. V. *Chem. Rev.* **2000**, *100*, 3009–3066.
(12) Kochi, T.; Noda, S.; Yoshimura, K.; Nozaki, K. *J. Am. Chem. Soc.* **2007**, *129*, 8948–8949.
(13) Luo, S.; Jordan, R. F. *J. Am. Chem. Soc.* **2006**, *128*, 12072–12073.
(14) Cabri, W.; Candiani, I. *Acc. Chem. Res.* **1995**, *28*, 2–7.
(15) The intermediately formed 2,1-insertion product was not fully characterized due to its low concentration. However, the formation of the β-hydride elimination product methyl crotonate together with a simultaneous decrease of a characteristic high-field triplet (0.3–0.5 ppm) unambiguously confirm the identity of this intermediate.
(16) (a) Becke, A. D. *Phys. Rev. A* **1988**, *38*, 3098–3100. (b) Perdew, J. P. *Phys. Rev. B* **1986**, *33*, 8822–8824. (c) Perdew, J. P. *Phys. Rev. B* **1986**, *34*, 7406–7406.
(17) (a) Guironnet, D.; Caporaso, L.; Neuwald, B.; Göttker-Schnetmann, I.; Cavallo, L.; Mecking, S. *J. Am. Chem. Soc.* **2010**, *132*, 4418–4426. (b) Noda, S.; Nakamura, A.; Kochi, T.; Chung, L. W.; Morokuma, K.; Nozaki, K. *J. Am. Chem. Soc.* **2009**, *131*, 14088–14100. (c) Haras, A.; Anderson, G. D. W.; Michalak, A.; Rieger, B.; Ziegler, T. *Organometallics* **2006**, *25*, 4491–4497.
(18) In line with Nozaki's results (ref 17b), the *trans*-coordinated intermediate is lower in energy than the *cis* intermediate for both complexes **2** and **9e**-MA. In detail, the *trans* intermediate is lower than the *cis* intermediate by about 42 and 69 kJ mol^{-1} for Pd-H complex **2** and complex **9e**-MA, respectively (Figure S7.7).
(19) Skupov, K. M.; Marella, P. R.; Simard, M.; Yap, G. P. A.; Allen, N.; Conner, D.; Goodall, B. L.; Claverie, J. P. *Macromol. Rapid Commun.* **2007**, *28*, 2033–2038.
(20) Piche, L.; Daigle, J.-C.; Poli, R.; Claverie, J. P. *Eur. J. Inorg. Chem.* **2010**, *29*, 4595–4601.
(21) Friedberger, T.; Wucher, P.; Mecking, S. *J. Am. Chem. Soc.* **2012**, *134*, 1010–1018.
(22) For characterization cf.: (a) Wehrmann, P.; Zuideveld, M.; Thomann, R.; Mecking, S. *Macromolecules* **2006**, *39*, 5995–6002. (b) Tritto, I.; Marestin, C.; Boggioni, L.; Zetta, L.; Provasoli, A.; Ferro, D. R. *Macromolecules* **2000**, *33*, 8931–8944.
(23) Skupov, K. M.; Marella, P. R.; Hobbs, J. L.; McIntosh, L. H.; Goodall, B. L.; Claverie, J. P. *Macromolecules* **2006**, *39*, 4279–4281.